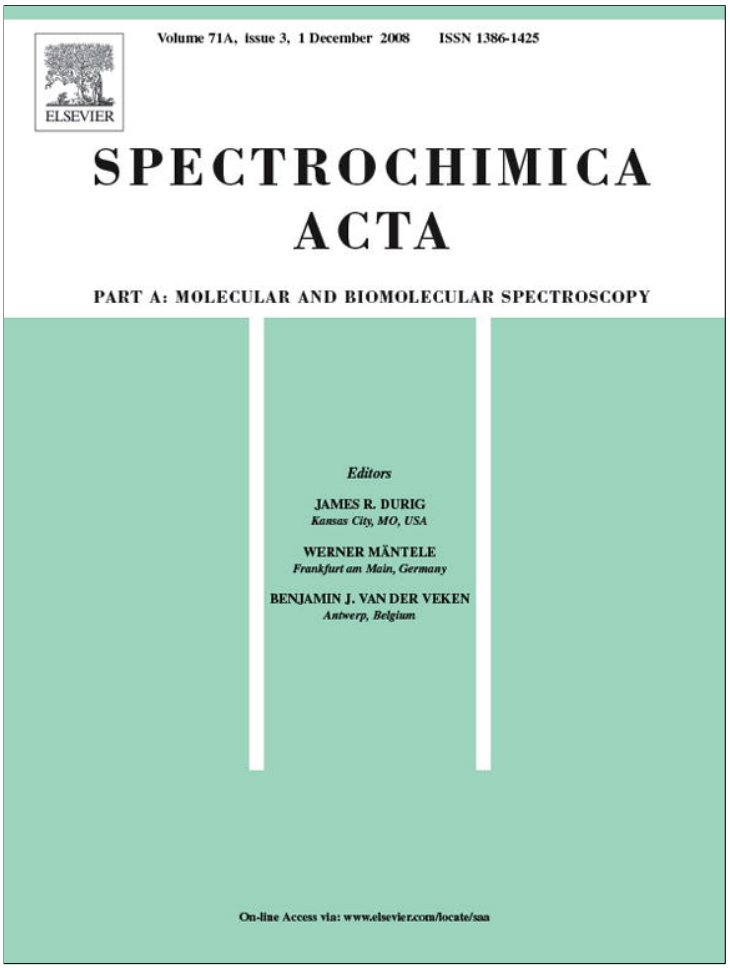

Spectrochimica Acta Part A 71 (2008) 975–983

Contents lists available at ScienceDirect

Spectrochimica Acta Part A: Molecular and Biomolecular Spectroscopy

journal homepage: www.elsevier.com/locate/saa

Biochemical properties of Cu/Zn-superoxide dismutase from fungal strain *Aspergillus niger* 26

Aleksandar Dolashki[a], Radoslav Abrashev[b], Stefan Stevanovic[c], Lilyana Stefanova[b], Syed Abid Ali[d], Ludmila Velkova[e], Rumyana Hristova[e], Maria Angelova[b], Wolfgang Voelter[a], Bart Devreese[f], Jozef Van Beeumen[f], Pavlina Dolashka-Angelova[e,*]

[a] *Interfacultary Institute of Biochemistry, University of Tübingen, Hoppe-Seyler-Straße 4, D-72076 Tübingen, Germany*
[b] *The Stephan Angeloff Institute of Microbiology, Bulgarian Academy of Sciences, G. Bonchev 26, 1113 Sofia, Bulgaria*
[c] *Department of Immunology, Institute for Cell Biology, University of Tübingen, Auf der Morgenstelle 15, D-72076 Tübingen, Germany*
[d] *H.E.J. Research Institute of Chemistry, International Center for Chemical and Biological Sciences, University of Karachi, Karachi-75270, Pakistan*
[e] *Institute of Organic Chemistry, Bulgarian Academy of Sciences, G. Bonchev 9, Sofia 1113, Bulgaria*
[f] *Laboratory of Protein Biochemistry and Protein Engineering, Ghent University, KL Ledeganckstraat 35, 9000 Ghent, Belgium*

ARTICLE INFO

Article history:
Received 15 December 2007
Received in revised form 3 February 2008
Accepted 13 February 2008

Keywords:
Aspergillus niger 26
Cu/Zn-superoxide dismutase
Mn-SOD
Fluorescence and CD spectroscopy

ABSTRACT

The fungal strain *Aspergillus niger* produces two superoxide dismutases, Cu/Zn-SOD and Mn-SOD. The primary structure of the Cu/Zn-SOD has been determined by Edman degradation of peptide fragments derived from proteolytic digests. A single chain of the protein, consisting of 153 amino acid residues, reveals a very high degree of structural homology with the amino acid sequences of other *Aspergillus* Cu/Zn-SODs. The molecular mass of ANSOD, measured by MALDI-MS and ESI-MS, and calculated by its amino acid sequence, was determined to be 15 821 Da. Only one Trp residue, at position 32, and one disulfide bridge were identified. However, neither a Tyr residue nor a carbohydrate chain occupying an N-linkage site (–Asn–Ile–Thr–) were found. Studies on the temperature and pH dependence of fluorescence, and on the temperature dependence of CD spectroscopic properties, confirmed that the enzyme is very stable, which can be explained by the stabilising effect of the disulfide bridge. The enzyme retains about 53% of its activity after incubation for a period of 30 min at 60 °C, and 15% at 85 °C.

1. Introduction

Exposure to radiation, ultraviolet light and chemical agents of tissues and cells results in the production of reactive oxygen species (ROS) such as the superoxide anions (O_2^-) and H_2O_2 [1,2] which are toxic to living organisms, causing oxidative damage to proteins, nucleic acids, and lipids [3]. Superoxide dismutases (SOD, E.C. 1.15.1.1) are a ubiquitous class of metalloenzymes that play a crucial role in protecting organisms against toxic effects caused by ROS [4,5]. Through means of a metal ion in their active sites, the enzymes rapidly convert two of the superoxide radicals to hydrogen peroxide and molecular oxygen [6,7]. SODs are classified into four groups depending on their metal cofactors: Mn-SOD [8], Cu/Zn-SOD [9,10], Fe-SOD [11] and Ni-SOD [12]. The Cu/Zn-SODs are typically found in the cytosol of eukaryotes, while Fe-SODs are mainly found in prokaryotes and chloroplasts and Mn-SODs occur in prokaryotes and mitochondria [13]. Cu/Zn-SODs were isolated and investigated from *Radix lethospermi* [14], a thermotolerant *Kluyveromyces* yeast strain [15], and the fungi *Aspergillus* [16], *Cordyceps militaris* [17], and *Humicola lutea* [18]. The three-dimensional structure of human Mn-SOD has been determined and compared with that of the homologous fungal *Aspergillus fumigatus* SOD [19]. Fe-SODs and Mn-SODs share a high degree of amino acid sequence homology [20], while CuZn-SODs represent a distinct class.

The genes of a variety of fungi have been made publicly available in databases. These include *sod1*, encoding a major Cu/Zn-SOD in *Neurospora crassa* [21], a *sod2* gene encoding Mn-SOD in *Penicillium chrysogenum* [22], *Aspergillus fumigatus* [23] and *Colletotrichum graminicola* [24], and *sod1* and *sod2* encoding a Cu/Zn-SOD and a Mn-SOD in *Saccharomyces cerevisiae*, respectively [25,26].

Abbreviations: ANSOD, superoxide dismutase from *Aspergillus niger*; DO, dissolved oxygen; E:S, enzyme:substrate; HIC, hydrophobic-interaction chromatography; HL-SOD, *Humicola lutea* SOD; HPLC, high performance liquid chromatography; FPLC, fast performance liquid chromatography; MALDI-MS, matrix-assisted laser desorption/ionization mass spectrometry; PAGE, polyacrylamide gel electrophoresis; ROS, reactive oxygen species; SOD, superoxide dismutase; TCA, trichloroacetic acid; NBT, nitroblue tetrazolium; TEMED, *N,N,N′,N′*-tetramethylethylenediamine.

* Corresponding author at: Institute of Organic Chemistry, Bulgarian Academy of Sciences, G. Bonchev 9, Sofia 1113, Bulgaria. Tel.: +359 2 9606163; fax: +359 2 8700225.
E-mail address: pda54@yahoo.com (P. Dolashka-Angelova).

1386-1425/$ – see front matter © 2008 Elsevier B.V. All rights reserved.
doi:10.1016/j.saa.2008.02.023

Aspergillus niger 26 is a useful model fungus for the study of the effects of environmental factors on the biosynthesis of a variety of enzymes, and is of interest to the biotechnological industry due to its ability to produce polymethylgalacturonase [27]. Oxygen, as a substrate for energy supply in bioreactor processes, and ROS arising from it play a central role in enzyme production. A study on the biosynthesis and biochemical properties of the antioxidant enzyme SOD in protecting *A. niger* 26 during growth is therefore of great importance. In the present paper, a study on the biochemical properties of Cu/Zn-SOD from *Aspergillus niger* strain 26 is carried out.

2. Materials and methods

2.1. Fungal strain, culture media and cultivation

We used the fungal strain *A. niger* 26, from the Mycological Collection of the Institute of Microbiology, Sofia, maintained at 4 °C on beer agar, pH 6.3. The composition of the culture medium AN-3 used for submerged cultivation was described earlier [29]. The cultivation was performed in a 3 or 12 l bioreactor ABR-09 (working volume 2 and 7 l, respectively), developed and constructed by the former Central Laboratory for Bioinstrumentation and Automatisation (CLBA) of the Bulgarian Academy of Sciences. The bioreactor was equipped with pH monitoring, automatic DO monitoring and a control system. For the inoculum, 80 ml of seed medium was inoculated with 5 ml of spore suspension, at a concentration of 2×10^8 spores/ml, in 500 ml Erlenmeyer flasks. The cultivation was performed on a shaker (220 rpm) at 30 °C for 24 h. The bioreactor cultures were performed with 8% (v/v) 24-h-old shake-flask inoculum at 30 °C for 72 h. The fermentation parameters were: impeller speed, 600 rpm, and air flow, 1 vvm (1 volume of air per 1 volume of liquid per min).

2.2. Purification of Cu/ZnSOD

2.2.1. Cell-free extract preparation

The cell-free extract was prepared as described earlier [28]. Briefly, mycelium biomass was harvested by filtration, washed with distilled water and then with cold 50 mM potassium buffer (pH 7.8), and resuspended in the same buffer. The cell suspension was disrupted by a homogenizer model ULTRA Turax T25 IKA. The temperature during treatment was maintained at 4–6 °C by chilling in an ice-salt bath and during filtration through filter paper. Cell-free extracts were clarified at 12 000 × *g* for 20 min at 4 °C. All further purification procedures were carried out at 4 °C.

2.2.2. Ammonium sulphate fractionation

The cell debris were removed by centrifugation (12 000 × *g*, 20 min, 4 °C). The resulting supernatant was brought to 30% saturation by gradually adding solid $(NH_4)_2SO_4$ and was stirred for 10–12 h at 4 °C. The precipitate was removed by centrifugation (12 000 × *g*, 20 min), dissolved in 20 mM Tris/HCl, pH 7.8, and dialyzed against the same buffer for 24 h at 4 °C.

2.2.3. Column chromatographic separations

The supernatant was directly applied to an Octyl-Sepharose column (40 mm × 32 mm) equilibrated with 20 mM Tris/HCl, pH 7.8, containing 30% ammonium sulphate. The column was washed thoroughly with 200 ml of equilibration buffer so that all unbound proteins were removed. The SOD containing fraction was directly applied on a Phenyl-Sepharose column (62 mm × 35 mm) equilibrated with 20 mM Tris/HCl, pH 7.8, speed 70 ml min^{-1} and washed until the absorbance at 276 nm reached a value of 0.1. SOD-containing fraction was then eluted with buffer containing 10% ammonium sulphate. Fractions of 6 ml were collected, and those containing SOD activity were pooled, concentrated by lyophilization and loaded onto a Q-Sepharose column of an FPLC system. The column was eluted with 50 mM Tris/HCl, pH 7.8, using a 0–0.1 M NaCl gradient for the first 20 min, followed by a 0.1–0.5 M NaCl gradient during the next 20 min, at a flow rate of 1 ml/min. A Mono Q column 5/5 was used for additional purification. Pure SOD was eluted at a flow rate of 1 ml/min using a 0–0.5 M NaCl gradient in 50 mM Tris/HCl.

2.3. Measurement of enzyme activity and protein amount

The SOD activity was measured by the nitroblue tetrazolium (NBT) reduction method of Beauchamp and Fridovich [30]. One unit of SOD activity was defined as the amount of SOD required to inhibit the reduction of NBT by 50%, measured at 560 nm, and was expressed as units per mg protein [U/mg protein]. Cyanide (5 mM) was used to distinguish between the cyanide-sensitive isoenzyme Cu/Zn-SOD and the cyanide-resistant Mn-SOD. The Cu/Zn-SOD activity was obtained as total activity minus the activity in the presence of 2 mM cyanide. Protein was estimated by the Lowry procedure [31], using crystalline bovine serum albumin as standard.

For the detection of SOD activity in gels, proteins were separated on an 8.5% non-denaturing PAGE and stained using NBT, riboflavin and TEMED, as previously described [30]. Potassium cyanide (KCN) was used at 10 mM to ascertain the SOD type.

2.4. Determination of molecular weight using different methods

2.4.1. Polyacrylamide gel electrophoresis (SDS-PAGE)

Subunit size was determined by SDS-PAGE according to Laemmli after boiling the proteins at 100 °C for 5 min in the presence of 2% SDS and 5% 2-mercaptoethanol [32]. Electrophoresis was on 10% acrylamide gels. Standards used were rabbit phosphorylase b (97.4 kDa), bovine serum albumin (66 kDa), rabbit actin (43 kDa), bovine carbonic anhydrase (31 kDa), trypsin inhibitor (20.1 kDa), and hen egg white lysozyme (14.4 kDa). Proteins were visualized by staining with Coomassie Brilliant Blue G-250.

2.4.2. Mass spectrometric analyses

Using MALDI-TOF MS, about 50 pmol of the HPLC fractions were dissolved in 0.1% (v/v) TFA and applied to the target of a 4700 Proteomics Analyser with TOF/TOF optics (Applied Biosystems, Framingham, MA). The matrix was α-cyano-4-hydroxycinnamic acid. A total of 4500 shots were acquired in the MS mode. Human albumin (66347.7 Da) was used to calibrate the mass scale.

For electrospray ionization mass spectrometry, mass spectra were acquired on the (ESI-MS) Q-TOF mass spectrometer (Micromass, Manchester, UK), equipped with a nanospray source. Protein samples were prepared by diluting the protein stock solution in 10 mM ammonium acetate buffer, pH 2.5. ESI source settings were kept constant throughout all measurements to avoid changes in the ion desorption and transmission. The spectra were acquired at a rate of 5 s. To ensure a high signal-to-noise ratio, typically 180–280 scans were averaged to generate each spectrum.

2.5. Pyridylethylation and enzymatic digestions of Cu/Zn-ANSOD

Two milligrams of Cu/Zn-ANSOD were dissolved in 1.0 ml of 0.25 M Tris/HCl, pH 8.5, 6 M guanidine–HCl, and 1 mM EDTA. An ethanolic solution of 2-mercaptoethanol (10%, v/v in water, at 100-fold molar excess to the cysteinyl residues) was added. The mixture was incubated under nitrogen for 2 h at room temperature in the dark. Neat 4-vinylpyridine (also 100-fold molar excess of the

expected cysteinyl residues) was added and the mixture was incubated under nitrogen for 2 h at room temperature in the dark. The pyridylethylated protein was desalted by reverse phase HPLC on an Aquapore RP-300 column (2.1 mm × 30 mm; Applied Biosystems, Weiterstadt, Germany).

Twenty microliters of the trypsin solution (1 mg/ml) was added to 0.50 ml of 25 mM Tris/HCl, pH 9.0, containing 1 mg carboxymethylated SOD (E:S 1:50); the reaction mixture was incubated overnight at room temperature. The digestion mixture was applied to an HPLC Hypersil column (250 mm × 4.6 mm; 5 μm HyPURITY C_{18}, Thermo Quest), eluted with eluent A (0.1% TFA in water) and eluent B (80% acetonitrile in A), using a gradient program of 0% B for 5 min and then 0–100% B in 60 min; the flow rate was 0.6 ml/min. The UV absorbance of the elution was monitored at 214 nm. Peak fractions were dried and after dissolving in 40% methanol/1% formic acid, they were subjected to automated Edman N-terminal sequencing (Procise 494A Pulsed Liquid Protein Sequencer, Applied Biosystems, Foster City, Ca).

2.6. Homology modeling of Cu/Zn-ANSOD

The three-dimensional structure of Cu/Zn-ANSOD was modeled using the crystal structure coordinates of yeast (*Saccharomyces cerevisiae* [33] Cu/Zn-SOD as a template (pdb i.d. code 1f1g, chain A), known to a resolution of 1.35 Å [34]. All steps of homology model building were performed by the program MODELER, version 6 [35,36]. Several rounds of model building were carried out to obtain the most plausible structure. Models were investigated with the graphics display program WebLab Viewer (v4.0) and/or SPDB Viewer (v3.7). The possible interactions were analyzed using the Whatif web-interface [37].

Assessment of the reliability of the predicted homology models of *Aspergillus* Cu/Zn-SOD was carried out by the ENERGY command of the program MODELLER and the programs PROSA and PROCHECK [35,38]. Furthermore, the variability among the models was compared by the superposition of C(-traces and backbones onto the template structure (pdb i.d. code 1f1g, 1jcw, 1jcv, 1yaz), their mutants (pdb i.d. code 1b4t, 1f18, 1f1a, 1f1d, etc.), and other related SOD structures from different origin (pdb i.d. code 1cbj, 1jk9, 1azv, 1l3n, 1ptz, etc.).

2.7. Effect of temperature and pH on Cu/Zn ANSOD activity

Enzyme activity of ANSOD was studied by incubating the enzyme at 5 °C temperature intervals from 25 to 85 °C, in 5 mM potassium phosphate, pH 7.8. Aliquots required for the assays were removed and immediately kept on ice for the determination of residual enzymatic activity.

The effect of pH on the activity of pure Cu/Zn-SOD was examined by enzyme incubation during different times (0.5–24 h) in 50 mM buffers at different pH values (pH 4.0–6.0, citric-citrate; pH 6.0–7.8, potassium phosphate; pH 7.8–8.8, Tris/HCl; pH 8.8–12, glycine/NaOH). The pH of the incubation mixtures was measured immediately after the addition of the enzyme and after different incubation times. The activity of the samples was assayed under standard conditions.

2.8. Stability of Cu/Zn ANSOD

2.8.1. Fluorescence measurements

Analyses were performed using a PerkinElmer model LS 5 spectrofluorimeter, equipped with a thermostatically controlled assembly and a data station model 3600. The excitation wavelength was 295 nm and emitted light intensity was integrated over the period of 1 s and detected at 295–450 nm.

Fluorescence quantum yields were determined by equation: $Q = Q_x(F_x/A_x)(A_{st}/F_{st})(\chi_x/\xi_{st})$ where Q_x, F_x and A_x are the emission quantum yield, the emission intensity at wavelength χ and the absorbance at the excitation wavelength, respectively, and F_{st} and A_{st} are the same parameters for the reference standard *N*-acetyltryptophanamide (Ac-Trp-NH_2) which has a quantum yield of 0.13 [39].

2.8.2. CD measurements

Circular dichroism was measured with a Jasco J-720 dichrograph, equipped with an IBM PC-AT, PS/2 personal computer, multiscan monitor CMS-3436, and a Hewlett-Packard colour graphics plotter model HP 7475A. Protein solutions in 50 mM Tris/HCl buffer, 10 mM $CaCl_2$, pH 8.0, were thermostatically controlled using a NESLAB thermostat model RTE-110, connected with a digital programming controller. The temperature inside the cuvette was monitored *via* a thermocouple.

2.8.3. Temperature stability

The temperature dependence of the SOD fluorescence was determined at pH 7.5 in 0.05 M Tris/HCl buffer. Some 0.2 mg of sample for CD and 0.1 mg for fluorescence analysis were kept for 10 min at the desired temperature prior to the measurement to ensure the attainment of thermal equilibration. The critical temperature (T_c) and melting temperature (T_m) values were calculated from the data of fluorescence spectroscopy or circular dichroism, respectively.

2.8.4. pH stability of Cu/Zn-SOD

The pH dependence of the stability of the Cu/Zn-SOD was determined for 0.1 mg/ml (for fluorescence measurements) and 0.2 mg/ml (for CD measurements) samples, kept for 10 min in 10 mM HEPES buffer at the desired pH values (pH 1.6–11.8).

3. Results and discussion

3.1. Purification of two isoenzymes

After the ammonium sulphate precipitation step, purification of SOD was achieved initially using HIC chromatography. The solute, eluted off the Octyl-Sepharose column with the void, was directly adsorbed on a Phenyl-Sepharose column. SOD was eluted using 10% ammonium sulphate. The purification on the Phenyl-Sepharose column revealed a single peak containing two SOD species with a combined specific activity of 66 U/mg protein (Table 1). The high volume of the sample (about 12 ml) and the high elution rate of 70 ml/h were used in this step for better purification. Compared to the standards on the native PAGE-electrophoregram, the two bands on Fig. 1, lane 3 were identified as Cu/Zn- and Mn-SOD, respectively.

Table 1
Purification scheme of *Aspergillus niger* 26 Cu/Zn-SOD

Purification step	Total protein (mg)	Total SOD activity (U)	Specific SOD activity (U mg^{-1})	Yield (%)	Purification (fold)
Crude extract	540	17800	33	100.0	1.00
Octyl-Sepharose	206	4620	22	26.0	n.a.
Phenyl-Sepharose	10.7	702	66	4.0	2.0
Q Sepharose	0.600	612	1020	3.4	7.5
Mono Q	0.200	588	2940	3.3	2.9

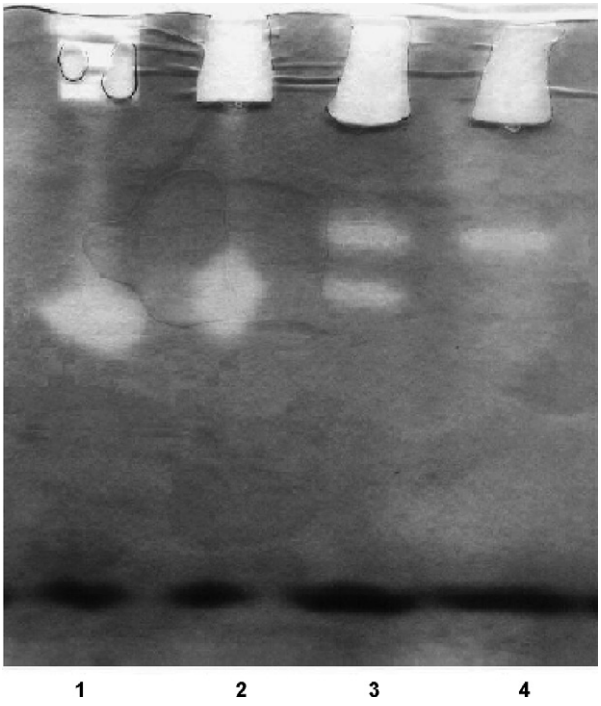

Fig. 1. SDS-PAGE of ANSODs at different steps of the purification procedure. Lane 1 – standard Cu/Zn-SOD *Humicola lutea* 103; lane 2 – *Aspergillus niger* Cu/Zn-SOD after purification by ion-exchange chromatography, using column Mono Q 5/5; lane 3 – *Aspergillus niger* Mn-SOD after purification on a Phenyl-Sepharose column; lane 4 – standard Mn-SOD *Humicola lutea* 110.

The isolated active fraction was pooled, concentrated by lyophilization and loaded onto a Q-Sepharose column (Fig. 2). After eluting the column with a nonlinear NaCl gradient, SOD active fractions were isolated, with a specific activity of 1020 U/mg protein (Table 1). The two enzymes were eluted together from the column resulting in a 7.5-fold increase in specific activity. The active fractions were concentrated by ultrafiltration over a PM-10 membrane and further purification was achieved on a second column (Mono Q 5/5; Fig. 3). Two fractions were isolated: one with a product of higher molecular mass containing Mn-SOD, and the second,

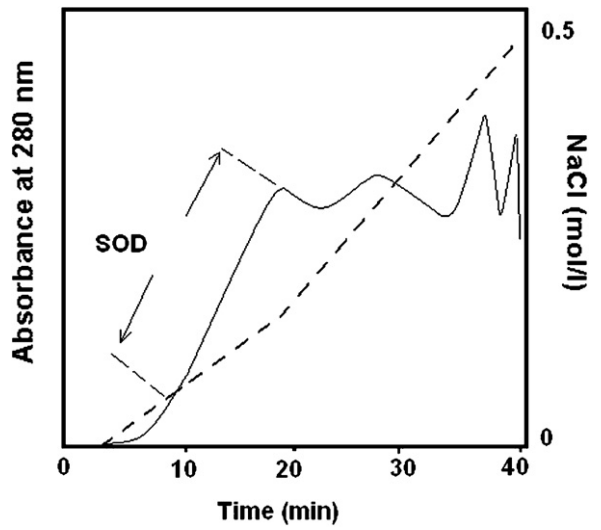

Fig. 2. Profile of SOD isolation on a Q-Sepharose column. The column was eluted at a flow rate of 1 ml/min with 50 mM Tris/HCl, pH 7.8, using a 0–0.5 M NaCl gradient (- - -).

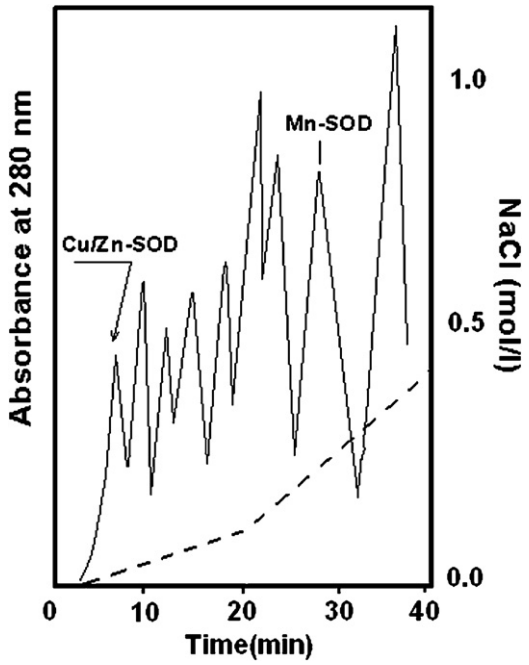

Fig. 3. Profile of SOD purification on a Mono-Q 5/5 column, eluted with 50 mM Tris/HCl and a 0–0.5 M NaCl gradient (- - -) a flow rate of 1 ml/min.

containing one Cu/Zn-SOD with lower mass and specific activity of 2940 U/mg protein (Fig. 1, lane 2). Direct evidence confirming the presence of both SODs was proven by *N*-terminal sequencing.

3.2. Molecular masses of Cu/Zn- and Mn-ANSODs

The molecular weight of Cu/Zn-ANSOD and Mn-ANSOD was determined through several methods. First, purified SODs were injected separately on a Hypersil C18 column, where one peak appeared for each fraction in the chromatograms, indicating that Cu/Zn-SOD and Mn-SOD (data not shown) obtained from the last step of purification were homogeneous.

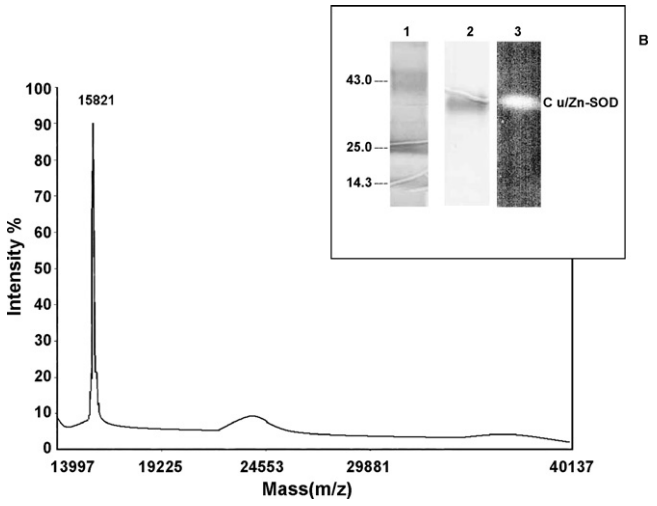

Fig. 4. Control of purity of purified *A. niger* Cu/Zn-SOD. A) native PAGE on a 12% gel of purified Cu/Zn- ANSOD; (Coomassie staining) lane 1 – standard, lane 2 – Cu/Zn-ANSOD, and (NBT staining) lane 3 – Cu/Zn-ANSOD; B) MALDI-TOF-MS, spectrum of Cu/Zn-SOD. Solutions of human albumin (66 347.7 Da) and rabbit actin (43 000 Da) were used to calibrate the mass scale.

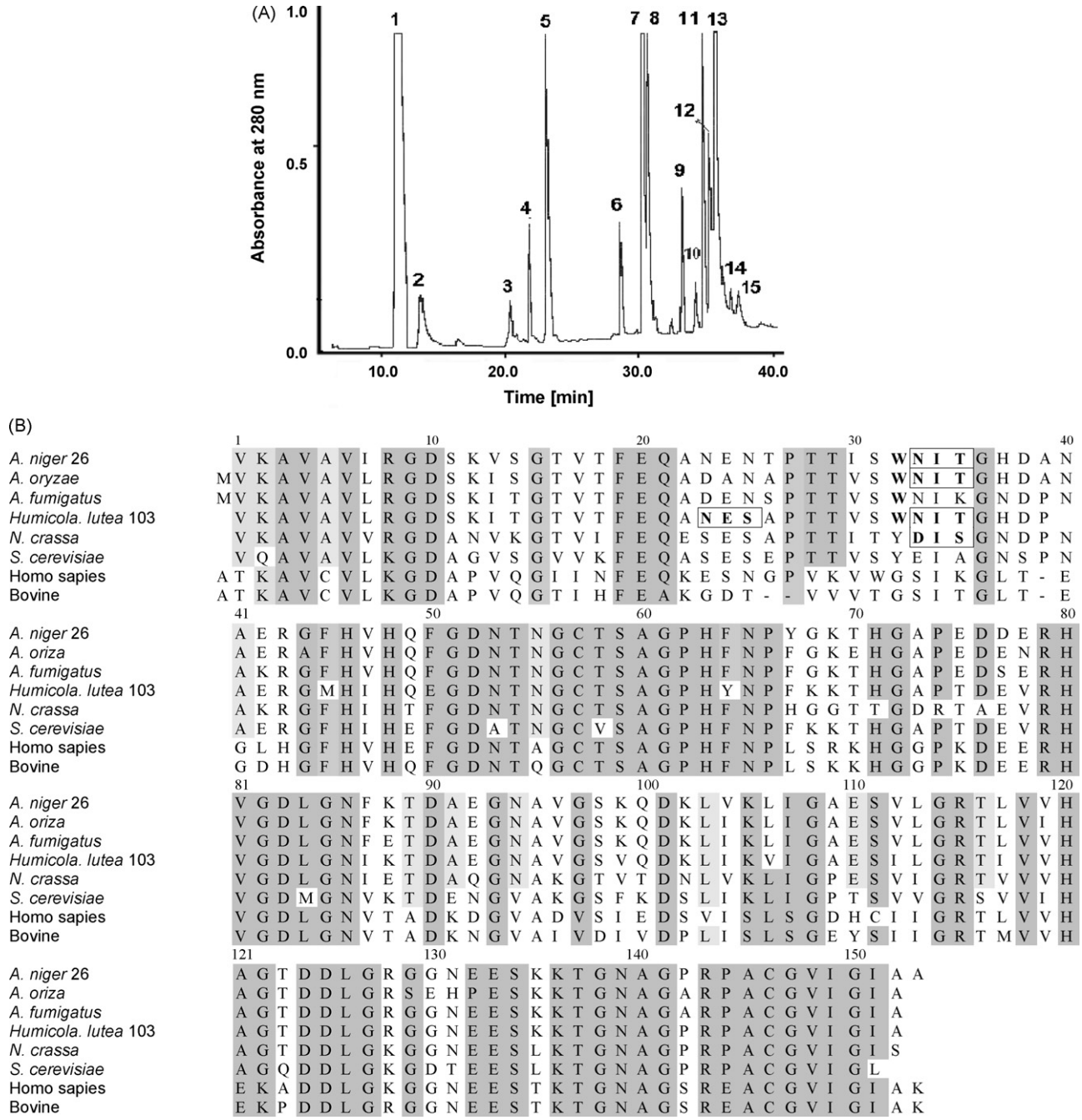

Fig. 5. (A) Reverse phase chromatography of tryptic peptides of Cu/Zn-AnSOD, separated on a HPLC Hypersil column (250 mm × 4.6 mm; 5 μm HyRURITY C18, Termo Quest), and eluted as given in Section 2; (B) complete amino acid sequence of Cu/Zn-ANSOD and sequence alignment with the Cu/Zn-SODs of *Aspergillus oryzae* (Q877B5), *Aspergillus fumigatus* (Q9Y8D9), *Humicola lutea* 103 (P83684) or *Neurospora crassa* (P07509) as well as from other species, such as yeast *S. cerevisiae* (P00445), *Homo sapiens* (P00441), bovine (1E9OA).

The rough masses of the *Aspergillus* Cu/Zn- and Mn-SODs were determined by PAGE to be 30 kDa (Fig. 4 insert) and 88 kDa, respectively. These values indicate that the enzymes are composed of dimers and tetramers, respectively, whose association depends upon noncovalent interactions. Using MALDI-TOF-MS, the exact molecular masses of both enzymes were determined, showing only one peak at 15 821 Da for Cu/Zn-SOD (Fig. 4) and a 22.340 kDa mass peak for Mn-SOD, indicating the presence of the monomers. These results were confirmed by the more sensitive electrospray ionization mass spectrometric method (15 824 Da for the structural subunit of Cu/Zn-SOD, data not shown).

3.3. Amino acid sequence of Cu/Zn-SOD

The primary structure of Cu/Zn-ANSOD was elucidated by N-terminal sequencing of the intact protein and amino acid sequence analysis of a set of HPLC-separated overlapping peptides (Fig. 5A). The masses of the peptides were also determined by MALDI-TOF-MS and found to be in good agreement with the theoretical masses calculated from the sequences.

A sequence alignment with other fungal Cu/Zn-SODs as well as with SOD from selected eukaryotic organisms is shown in Fig. 5B aided by the programme LALIGN. At the acidic pH of 0.1% (v/v) TFA,

the homodimer ANSOD dissociates into monomers of 153 amino acid residues, which is very close to the 152 amino acid residues of HL-SOD (Mw = 15 716 Da). The high similarity with the sequences of other fungal Cu/Zn-SODs amounts to 88% with the *Aspergillus oryzae*, 90% with that of *Aspergillus fumigatus*, 86% with *Humicola lutea* 103 and 74% with *Neurospora crassa*. The similarity is clearly smaller for SODs from the species *S. cerevisiae* (68%), *Homo sapiens* (58%) and Bovine (60%).

The three-dimensional structure of ANSOD was modelled using the program MODELLER and homologous *Saccharomyces cerevisiae* Cu/Zn-SOD as template. The stereochemical quality of the structure was checked by analyzing the modelled structure of fungal SOD by program PROCHECK (C) [38]. The geometric distribution of 91% of the amino acid residues is in the most favored regions and 9% in additionally allowed regions. The SOD molecule has a highly conserved typical structural scaffold common to all SODs with mainly antiparallel β-sheets connected by long variable loops and very short 3_{10}-helices (Fig. 6A). The two Cys residues, at positions 58 and 147, form a disulfide bond, as occurs in various Cu/Zn-SODs. Also the amino acid residues His46, 48, 63, 71, 80, and 120, and Asp83 in the active site (Fig. 6B) are conserved as in other Cu/ZnSODs.

The only tryptophan residue of the polypeptide chain (marked in red in the model), at position 32, is at the same position as in the fungal SODs of *A. niger*, *A. oriza*, *A. fumigatus* and *H. lutea*, but it is substituted by a tyrosine residue in the enzymes from of *N. crassa* and *S. cerevisiae*. The presence of Trp32 in Cu/Zn-ANSOD is responsible for the absorbance at 280 nm in the ultraviolet region and for the fluorescence emission at 310–450 nm in the fluorescence spectrum. Another similarity between fungal Cu/Zn-SODs (Fig. 5B) is the observation of one N-linkage site (–Asn–Ile–Thr–) at position 33–35 suggests that the enzyme might be glycosylated, as was found in HL-SOD [28]. However, the orcinol/sulphonic test to identify glycosylation of the ANSOD enzyme was negative, confirming that no glycan is bound to the glycosylated site in Cu/Zn-ANSOD.

3.4. Mn-SOD

As in the fungal strains *Humicola lutea* 110 and 103, also the Mn-SOD occurs in *Aspergillus niger* 26 strain [8,40]. Identification of this enzyme was performed by alignment of the N-terminal sequence with that of Mn-SODs from different species. As shown in Fig. 7, very high homology was observed in the conserved regions 4–5, 13–16, 26–27 and 30–35 with Mn-ANSODs (XP751672), *A. niger* (AAU4413), *A. flavius* (AAT81154), *A. oryzae* (BAE58164.1), *E. coli* (P00448) and bacterial SOD (P00449), on top of the identity of the residues 7,9,11 and 23.

3.5. Effect of pH and temperature on Cu/Zn-ANSOD activity

The effect of pH at 25 °C on the purified enzyme is shown in Fig. 8A. Optimum SOD activity was obtained at pH 6.2. The enzyme retains more than 90% of its activity after incubation in the buffer between pH 5.6 and 7.5, but it is inactivated by nearly 15% at pH 4 and it retains more than 60% of its activity up to pH 12.

The enzyme activity of Cu/Zn-ANSOD at different temperatures was examined at pH 7.8. The enzyme keeps its activity in the range from 25 to 45 °C (date are not shown), but was inactivated to 46% at 60 °C and to 85% after incubation for 30 min at 85 °C. The enzyme is more thermostable than the SODs from *A. nidulans* and *A. terreus* which lose significant activity at the higher temperatures [16]. Also HL-SOD [18] and the enzyme from *A. fumigatus* retain their activity up to 37 °C, but rapidly lose it at higher temperatures [16].

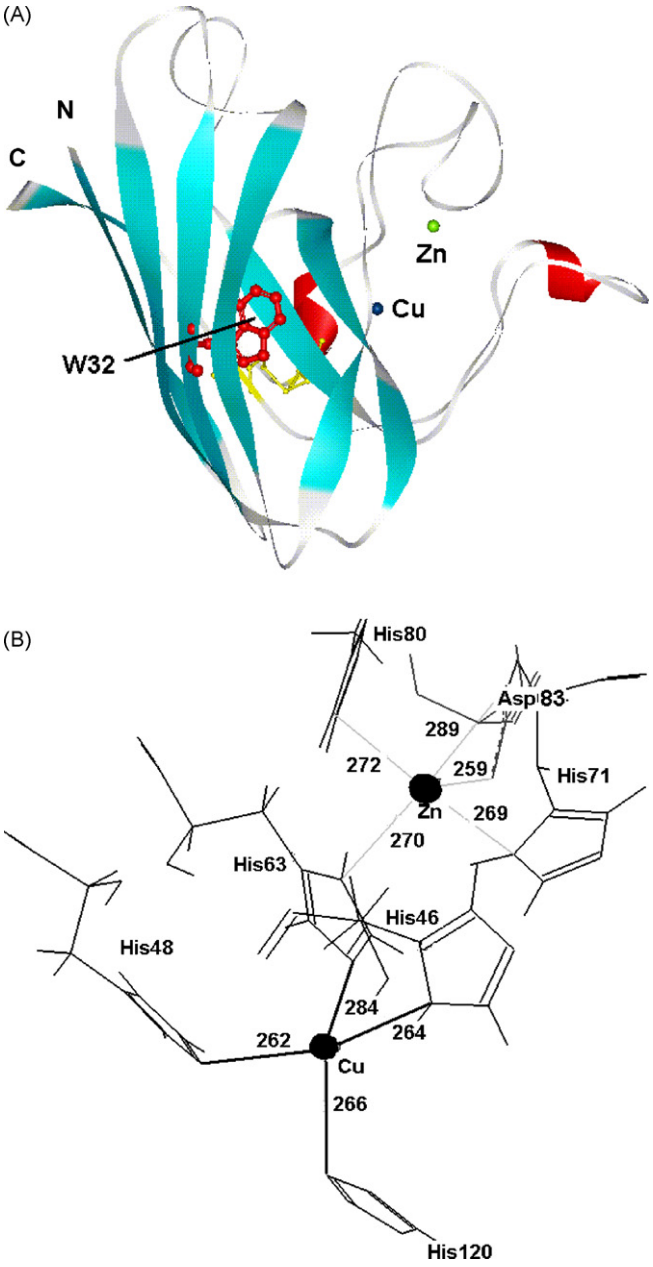

Fig. 6. (A) Ribbon presentation of the three-dimensional structural model of *Aspergillus niger*, Cu/ZnSOD established by the program MODELER. Antiparallel beta-sheets (cyan), connected by long variable loops (silver) are stabilized by one SS bridge between Cys57 and Cys146 (yellow). Active site Cu (blue) and Zn (green), and the buried Trp32 (red) as well as N- and C-terminus are also marked. (B) Map of active site of the fungal SOD depicting the coordination of Cu and Zn with the protein amino acid residues His46, 48, 63, 71, 80, and 120 and Asp83. The bond distances in Angström (Å) are calculated (For interpretation of the references to colour in this figure legend, the reader is referred to the web version of the article).

3.6. Effect of pH and temperature on the stability of Cu/Zn-ANSOD

We characterized the properties of Cu/Zn-ANSOD using the very sensitive method of fluorescence spectroscopy. Experiments were performed in 50 mM Tris/HCl buffer at an excitation wavelength of 295 nm, where at least 93% of the incident light is absorbed by the tryptophan residue in the protein. The presence of only one Trp, at position 32, and of no Tyr residues, was confirmed by the fact that the calculated transfer of energy from a Tyr to a Trp residue was found to be only 0.5%. In comparison, 30% energy transfer

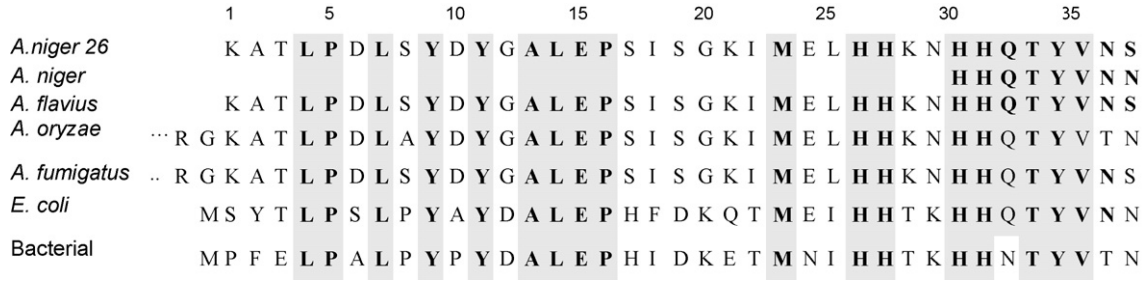

Fig. 7. N-terminal sequence of isolated Mn-SOD and comparison with those from other species: *A. fumigatus* (XP751672), *A. niger* (AAU4413), *A. flavius* (AAT81154), *A. oryzae* (BAE58164.1), *E. coli* (P00448) and bacterial SOD (P00449).

Table 2
Spectroscopic properties of Cu/Zn-SOD from *Aspergillus niger* 26

Cu/Zn-SOD	Emission λ_{max} (nm) at 295 nm	Quantum yield (Q, mol^{-1})	Critical temperature (T_c)	Melting temperature (T_m)
H. lutea 110				
holo-	328	0.010	–	69
apo-	338	0.051	68	61
A. niger 26				
holo-	343	0.019	61	65
apo-	346	0.057		58

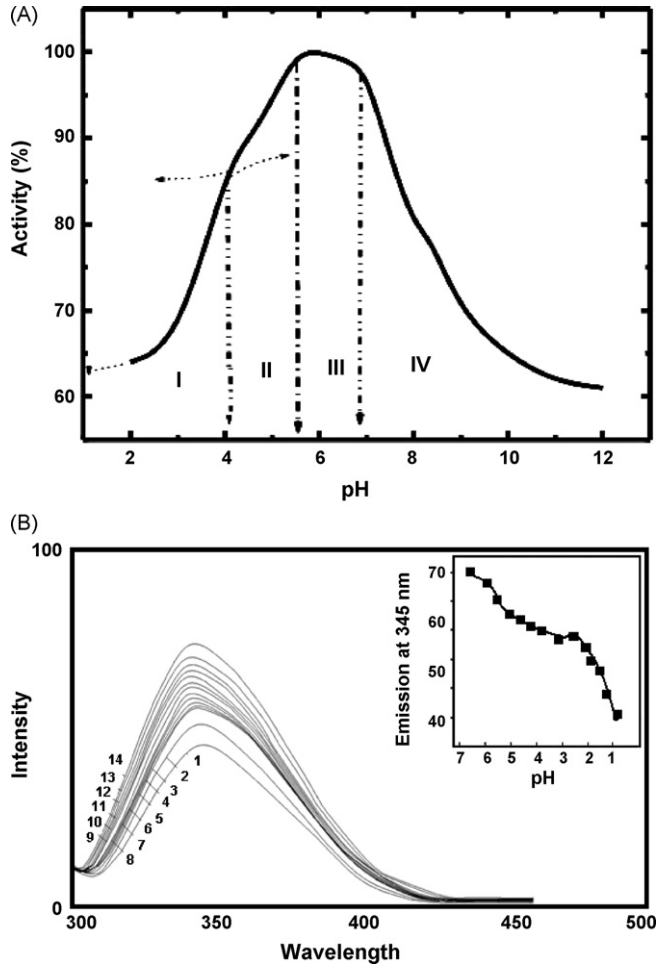

Fig. 8. (A) The effect of pH on the activity of the purified Cu/Zn-ANSOD (see Section 2). (B) The effect of pH on the stability of the purified Cu/Zn-ANSOD using fluorescence spectroscopy (see Section 2). The numbers in the figure refer to the pH values.

is found in HL-SOD which contains one Tyr, aside from Trp32. Oxy-ANSOD exhibits an emission spectrum with a maximum at 343 nm (Table 2) which is a typical maximum for the tryptophyl side chain being in a polar environment. These results are different from the values found for the HL-SOD (328 nm) [28]. The emission wavelength maximum increases by 3 nm, comparing the oxy- with the apo-ANSOD, which suggests that the removal of copper slightly changes the environment of the tryptophan residues. In addition, the quantum yield increases three times (from $Q = 0.019$ for the oxy-form to $Q = 0.057$ for the apo-form) what can be explained by the longer distance between the Cu ion and Trp32.

3.6.1. *pH stability Cu/Zn ANSOD*

Since the quenching effect of the Cu ion in the active site on the Trp fluorescence is a function of pH, the experiments have been carried out on the apo-protein in order to avoid the complications due to the change in fluorescence intensity. The fluorescence spectra of apo-ANSOD were recorded at different pH values (Fig. 8B, main figure). The pH dependence of the Trp-fluorescence quantum yield (Q) of apo-ANSOD in the acidic region is shown in Fig. 8B (inset), from which the pK values could be calculated to be 1.7 and 4.8. The first value is tentatively assigned to acid denaturation, which could be proven by CD measurements. The Q-change with p$K = 4.8$ may be correlated with the ionization of a single carboxyl group. There was no change in Q behaviour in the neutral pH region (6.5–8.5). An 'alkaline ionization' with a p$K = 10.7$ is obviously connected with the alkaline denaturation (data are not shown).

3.6.2. *Thermostability of Cu/Zn-ANSOD*

The temperature dependence of the intensity of the emission was determined in the range from 20 to 95 °C in 50 mM Tris/HCl, 10 mM $CaCl_2$, pH 7.5 buffer. The data were collected for the apo-forms only, because oxygen saturation of Cu-containing proteins is temperature-dependent. The Arrhenius plot for the apo-form of ANSOD is shown in Fig. 9A. The critical temperature value T_c was found to be 61 °C, which indicates that ANSOD is nearly as stable as HLSOD ($T_c = 68$ °C) (Table 2). As the thermal denaturation of this protein is irreversible after passing the T_c, equilibrium thermodynamic parameters were not determined.

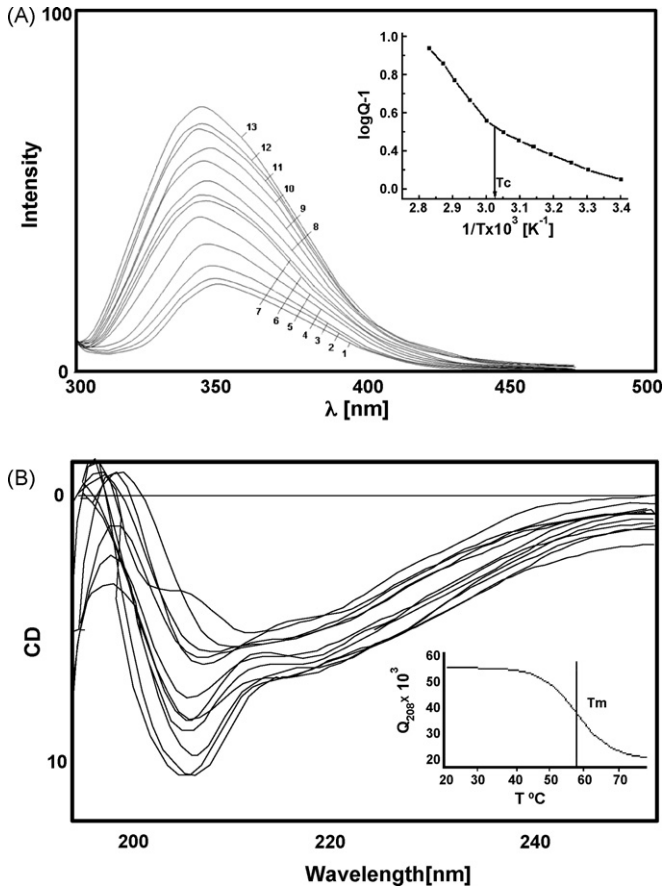

Fig. 9. Thermal stability of ANSOD investigated using: (A) Fluorescence spectroscopy and deduced critical temperature (T_c); (B) CD spectroscopy and deduced melting temperature (T_m) (see Section 2).

The thermal stability of ANSOD was also investigated using CD spectroscopy. The far-ultraviolet CD spectrum of the enzyme is dominated by the negative band at 208 nm, which is mainly correlated with the β-sheet structure (Fig. 9B). This is in agreement between the secondary structural contents of *Humicola lutea* SOD [18]. The CD spectra of the oxy- and apo-form of ANSOD were recorded in the temperature interval from 20 to 90 °C. From the sigmoidal curves, a melting temperature of 58 °C at the midpoint in the denaturation curve could be calculated, which is in a good agreement with the 61 °C obtained by fluorescence spectroscopy.

4. Conclusion

Two SODs were identified in the fungal strain *Aspergillus niger* 26. One is a member of the Cu/Zn-SOD family and the second one is a Mn-SOD. The specific activities of the Cu/Zn-SOD described here is broadly comparable with previously described Cu/Zn-SODs [16]. In addition, Cu/Zn-SOD isolated from *A. niger* strains are homodimers, with monomeric subunits of 15 821 Da. Mn-SOD exists in very small amount in its intact form as a tetramer with molecular mass of 22 340 Da per subunit.

The three-dimensional model of ANSOD shows a highly conserved and typical structural scaffold common to all SODs, including two Cys residues, at positions 58 and 147, which form a disulfide bond. There is only one tryptophan residue, at position 32, and one N-linkage site which, however, does not have a glycan linked.

The Cu/Zn-ANSOD is a stable enzyme, retaining its activity after incubation at pH values between 6 and 9 and keeping 100% of its activity at 45 °C compared to 20 °C. In contrast, *A. terreus* and *A. nidulans* Cu/Zn-SODs retain only 70 and 12%, respectively, of their 20 °C activity at 37 °C.

More precise information on the stability of the Cu/Zn-ANSOD proteins was obtained studying the kinetics of protein unfolding under the destabilizing conditions of pH variance and increasing temperature. The presence of two or three unfolding kinetic phases for holo- and apo-SOD indicates that, regardless of the presence of metals, the unfolding mechanism of SOD is not a simple transition from the native dimer to the unfolded monomer. In principle, this may be due to two conformational events: first, by the conformational changes in the dimer, followed by the dissociation to monomers, and subsequent by monomer unfolding. Since metal ligands are known to be lost at pH 2.0, conformational unfolding events for holo-SOD may be coupled to a loss of metal binding. The conformational dynamics of ANSOD correlates to that of *H. lutea* Cu/Zn-SOD studied by electrospray ionization mass spectrometry [40].

The effect of temperature, examined by fluorescence and CD spectroscopy showed that the values of T_c and T_m reflect the stability of the Cu/Zn-ANSOD, as is the case of HL-SOD.

Acknowledgement

This work was supported by the NCSI of the Ministry of Education and Science, Bulgaria (grant K-1401/04), which is greatly acknowledged.

References

[1] J.M. McCord, I. Fridovich, J. Biol. Chem. 244 (1969) 6049–6055.
[2] I. Fridovich, Toxicology 23 (1983) 239–257.
[3] J.S. Valentine, D.L. Wertz, T.J. Lyons, L. Liou, J.J. Goto, E.B. Gralla, Curr. Opin. Chem. Biol. 2 (1998) 253–262.
[4] I. Fridovich, J. Biol. Chem. 272 (1997) 18515–18517.
[5] H.M. Hassan, C.S. Moody, in: G. Rotilio (Ed.), Elsevier Science Publisher, New York, pp. 274–279, 1986.
[6] I. Fridovich, Annu. Rev. Biochem. 44 (1975) 147–159.
[7] I. Fridovich, Adv. Enzymol. Relat. Areas Mol. Biol. 58 (1986) 61–67.
[8] P. Dolashka-Angelova, L. Genova, S. Stoeva, B. Stefanov, M. Angelova, R. Hristova, S. Pashova, W. Voelter, J. Peptide. Res. 54 (1999) 279–289.
[9] P. Dolashka-Angelova, M. Angelova, L. Genova, S. Stoeva, W. Voelter, Spectrochim. Acta A. Mol. Biomol. Spectrosc. 55A (1999) 2249–2260.
[10] Z. Wang, Z. He, Q. Shen, Y. Gu, S. Li, Q. Yuan, J. Chromatogr. B: Anal. Technol. Biomed. Life Sci. 826 (1–2) (2005) 114–121.
[11] F.J. Yost, I. Fridovich, J. Biol. Chem. 248 (1973) 4905–4908.
[12] H.D. Youn, E.J. Kim, J.H. Roew, Y.C. Hah, S.O. Kang, Biochem. J. 318 (1996) 889–896.
[13] E. Fréalle, C. Noël, E. Viscogliosi, D. Camus, E. Dei-Cas, L. Delhaes, FEMS Immunol. Med. Microbiol. 45 (2005) 411–422.
[14] N.I. Haddad, Q. Yuan, J. Chromatogr. B. Anal. Technol. Biomed. Life Sci. 818 (2005) 123–131.
[15] A. Kujumdzieva, T. Nedeva, M. Morfova, V. Savov, J. Cult. Collections 2 (1997–1998) 44–50.
[16] M.D. Holdom, R.J. Hay, A.J. Hamilton, Infect Immun. 64 (1996) 3326–3332.
[17] Z. Wang, Z. He, S. Li, Q. Yuan, Enzyme Microb. Technol. 36 (2005) 862–869.
[18] P. Dolashka-Angelova, S. Stevanovic, A. Dolashki, M. Angelova, J. Serkedjieva, E. Krumova, S. Pashova, S. Zacharieva, W. Voelter, Biochem. Biophys. Res. Commun. 317 (2004) 1006–1016.
[19] S. Flückiger, P.R.E. Mitt, L. Scapozza, H. Fijten, G. Folkers, M.G Grütter, K. Blaser, R. Crameri, J. Immunol. 168 (3) (2002) 1267–1272.
[20] M.W. Parker, C.C. Blake, FEBS Lett. 229 (1988) 337–382.
[21] P. Chary, D. Dillon, A.L. Schroeder, D.O. Natvig, Genetics 137 (1994) 723–730.
[22] B. Díez, C. Schleissner, M.A. Moreno, M. Rodríguez, A. Collados, J.L. Barredo, Curr. Genet. 33 (1998) 387–394.
[23] R. Crameri, A. Faith, S. Hemmann, R. Juassi, C. Ismail, G. Menz, K. Blaser, J. Exp. Méd. 184 (1996) 265–270.
[24] G.-C. Fang, R.M. Hanau, L.J. Vaillancourt, Fungal Genet. Biol. 36 (2002) 155–165.
[25] E.C. Chang, D.J. Kosman, J. Bacteriol. 172 (1990) 1840–1845.
[26] E.C. Chang, B. Crawford, Z. Hong, T. Bilinski, D.J. Kosman, J. Biol. Chem. 266 (1991) 4417–4424.
[27] L. Slokoska, M. Angelova, Z. Naturforsch. 53C (1998) 968–972.

[28] M. Angelova, P. Dolashka-Angelova, E. Ivanova, J. Serkedjieva, L. Slokoska, S. Pashova, R. Toshkova, S. Vassilev, I. Simeonov, H.J. Hartmann, S. Stoeva, U. Weser, W. Voelter, Microbiology 147 (2001) 1641–1650.
[29] R. Abrashev, P. Dolashka-Angelova, R. Hristova, L. Stefanova, M. Angelova, J. Appl. Microbiol. 99 (2005) 902–905.
[30] C. Beauchamp, I. Fridovich, Anal. Biochem. 44 (1) (1971) 276–287.
[31] O.H. Lowry, H.J. Rosenbrough, A.L. Faar, R.J. Randall, J. Biol. Chem. 193 (1951) 265–275.
[32] U.K. Laemmli, Nature 227 (1970) 680–685.
[33] K. Djinovic, G. Gatti, A. Coda, L. Antolini, G. Pelosi, A. Desideri, M. Falconi, F. Marmocchi, G. Rotilio, M. Bolognesi, J. Mol. Biol. 225 (1992) 791–809.
[34] H.M. Berman, J. Westbrook, Z. Feng, G. Gilliland, T.N. Bhat, H. Weissig, I.N. Shindyalov, P.E. Bourne, The Protein Data Bank Nucl. Acids Res. 28 (2000) 235–242.
[35] A. Šali, T.L. Blundell, J. Mol. Biol. 2 (1990) 403–428.
[36] A. Šali, T.L. Blundell, J. Mol. Biol. 234 (1993) 779–815.
[37] R.W.W. Hooft, C. Sander, G. Vriend, Proteins 26 (1996) 363–376.
[38] R.A. Laskowski, M.W. McArthur, D.S. Moss, J.M. Thornton, J. Appl. Crystallogr. 26 (1993) 283–291.
[39] S.S. Lehrer, Biochemistry 10 (1971) 3254–3263.
[40] E. Krumova, P. Dolashka-Angelova, S. Pashova, L. Stefanova, J. Van Beeumen, S. Vassilev, M. Angelova, Enzyme Microb. Technol. 404 (2007) 524–532.